Title
Broad-Spectrum Kinase Profiling in Live Cells with Lysine-Targeted Sulfonyl Fluoride Probes

Journal
Journal of the American Chemical Society, 139(2)

ISSN
0002-7863

Authors
Zhao, Qian
Ouyang, Xiaohu
Wan, Xiaobo
et al.

Publication Date
2017-01-18

DOI
10.1021/jacs.6b08536

Peer reviewed

HHS Public Access

Author manuscript

J Am Chem Soc. Author manuscript; available in PMC 2018 March 19.

Published in final edited form as:

J Am Chem Soc. 2017 January 18; 139(2): 680–685. doi:10.1021/jacs.6b08536.

Broad-Spectrum Kinase Profiling in Live Cells with Lysine-Targeted Sulfonyl Fluoride Probes

Qian Zhao[†,‡,⊥], **Xiaohu Ouyang**[†,⊥], **Xiaobo Wan**[†], **Ketan S. Gajiwala**[‖], **John C. Kath**[‖], **Lyn H. Jones**[§], **Alma L. Burlingame**[‡], and **Jack Taunton**[*,†]

[†]Department of Cellular and Molecular Pharmacology, University of California, San Francisco, California 94158, United States

[‡]Pharmaceutical Chemistry, University of California, San Francisco, California 94158, United States

[§]Medicine Design, Pfizer, Cambridge, Massachusetts 02139, United States

[‖]Worldwide Research and Development, Pfizer, San Diego, California 92121, United States

Abstract

Protein kinases comprise a large family of structurally related enzymes. A major goal in kinase-inhibitor development is to selectively engage the desired kinase while avoiding myriad off-target kinases. However, quantifying inhibitor interactions with multiple endogenous kinases in live cells remains an unmet challenge. Here, we report the design of sulfonyl fluoride probes that covalently label a broad swath of the intracellular kinome with high efficiency. Protein crystallography and mass spectrometry confirmed a chemoselective reaction between the sulfonyl fluoride and a conserved lysine in the ATP binding site. Optimized probe 2 (XO44) covalently modified up to 133 endogenous kinases, efficiently competing with high intracellular concentrations of ATP. We employed probe 2 and label-free mass spectrometry to quantify intracellular kinase engagement by the approved drug, dasatinib. The data revealed saturable dasatinib binding to a small subset of kinase targets at clinically relevant concentrations, highlighting the utility of lysine-targeted sulfonyl fluoride probes in demanding chemoproteomic applications.

Graphical abstract

[*]**Corresponding Author:** jack.taunton@ucsf.edu.

[⊥]**Author Contributions**

Q.Z. and X.O. contributed equally.

Supporting Information

The Supporting Information is available free of charge on the ACS Publications website at DOI: 10.1021/jacs.6b08536.

Additional tables (XLSX)

Additional figures, detailed experimental methods including synthesis and characterization of new compounds, and X-ray data collection and refinement statistics (PDF)

ORCID

Jack Taunton: 0000-0002-9627-5898

Notes

The authors declare the following competing financial interest(s): K.S.G., J.C.K., and L.H.J. are employees and shareholders of Pfizer.

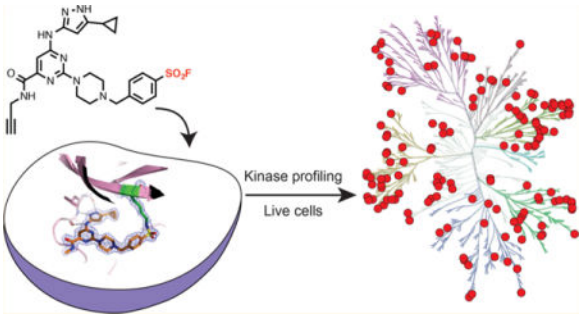

INTRODUCTION

Phosphorylation of serine, threonine, and tyrosine by protein kinases plays a central role in signal transduction and cellular physiology. Because aberrant kinase signaling has been implicated in many human diseases, selective kinase inhibitors have broad therapeutic potential.[1] With few exceptions, kinase inhibitors compete with ATP for binding to the active site, which is highly conserved among 518 human protein kinases. Because off-target kinase inhibition can lead to spurious mechanistic conclusions,[2] as well as toxic side effects, it is imperative to gain a quantitative understanding of kinase-inhibitor engagement, ideally in the context of living cells.

High-throughput methods for profiling kinase inhibitors typically rely on enzymatic activity or competition binding measurements with isolated kinases or kinase domains.[3,4] A potential limitation of these assays is that they are removed from the cellular environment, where dynamic interactions with regulatory proteins and lipids can modulate the conformation, catalytic activity, and subcellular localization of native protein kinases. Recently, chemoproteomic methods have been developed to quantify inhibitor binding to endogenous kinases in complex cellular proteomes. In these competition-based assays, reversible bead-immobilized kinase inhibitors[5–9] (“kinobeads”) or irreversible ATP-biotin probes[10,11] are employed to capture kinases for mass spectrometry analysis. While both platforms are major technological advances and can interrogate 150–200 endogenous kinases from a single cell line, neither kinobeads nor ATP-biotin probes are cell permeable. This lack of cell permeability is an intrinsic physicochemical property that cannot realistically be improved. As a consequence, dilute ATP-depleted lysates are prepared before the kinase-binding probes are added. This results in membrane dissolution and dilution of protein complexes, potentially altering the activation state and conformation of protein kinases. The most effective cell-permeable pan-kinase probes reported to date employ a photoreactive diazirine and can detect up to 22 intracellular kinases.[12,13] In this study, we report the first chemoproteomic probes that can capture up to 133 kinases from a single cell line, enabling broad-spectrum assessment of kinase-inhibitor occupancy in live cells.

RESULTS AND DISCUSSION

Sulfonyl fluorides are hydrolysis-resistant electrophiles that can react with diverse protein nucleophiles in a context-dependent manner.[14,15] Despite their attractive properties, sulfonyl fluorides have rarely been exploited in the structure-based design of lysine-targeted covalent

inhibitors.[16] Inspired by classical sulfonyl fluoride-based affinity probes,[17] we previously designed a 5′-fluorosulfonylbenzoyl nucleoside probe that covalently modifies SRC-family kinases and, possibly, other kinases with a small residue (e.g., threonine) in the "gatekeeper" position of the ATP-binding site.[18] Unlike FSBA (5′-fluorosulfonylbenzoyl adenosine), our sulfonyl fluoride probe potently and irreversibly inhibits endogenous SRC-family kinases in intact cells. To expand beyond this limited subset of kinases, we designed a new series of probes based on the pyrimidine 3-aminopyrazole scaffold shown in Figure 1A. This scaffold can form 3 hydrogen bonds with the conserved hinge region and has been shown to inhibit many kinases,[19,20] including kinases with bulky gatekeeper residues (phenylalanine, methionine, and leucine). By analyzing cocrystal structures of pyrimidine 3-aminopyrazoles bound to various kinases (PDB codes: 4b8m, 2f4j, 3f6x, 3ggf, 3soc, 2vn9, and 2uv2), we surmised that a short linker (3–5 Å) attached to the pyrimidine at C2 would optimally position a phenylsulfonyl fluoride proximal to the catalytic lysine. These considerations led to the design of the clickable piperazine-linked probes 1–3 (Figure 1A), in which the conformational flexibility and orientation of the phenylsulfonyl fluoride substituent were varied.

SRC was selected as a model kinase to assess covalent Lys modification. After incubating purified SRC kinase domain (5 μM) with probes 1–3 (15 μM) for 1 h, LC–MS analysis revealed formation of a 1:1 SRC adduct corresponding to the molecular mass of the probe with loss of fluoride (Figure S1). Whereas probes 1 and 2 reacted with SRC in quantitative yield, probe 3 achieved only ~30% labeling, suggesting suboptimal orientation of the *meta*-substituted sulfonyl fluoride. Previous studies have shown that sulfonyl fluorides can react with tyrosine as well as lysine residues.[14,21,22] Despite having 16 lysines and 13 tyrosines, most of which are solvent accessible, superstoichiometric labeling of SRC by the sulfonyl fluoride probes (3 equiv) was not observed. Specific modification of SRC at Lys295, corresponding to the catalytic lysine, was confirmed for probe 2 by trypsinization of the adduct, followed by LC–MS/MS analysis (Figure S2). Additionally, we obtained a 2.5 Å resolution cocrystal structure of SRC modified by probe 2 (Figure 1B). Consistent with previous kinase structures bound to related scaffolds, the 3-aminopyrazole of 2 interacts with SRC via 3 hydrogen bonds along with extensive van der Waals contacts. Unique to our structure is the presence of contiguous electron density between the phenylsulfonyl moiety and the side chain amine of Lys295, consistent with the LC–MS analysis. To test whether probe 2 can react specifically with the catalytic Lys of other kinases, we solved a second cocrystal structure (1.6 Å resolution) with the EGFR kinase domain (Figure 1C). Notably, the position of the ligand and the modified Lys side chain are precisely aligned in the two structures (Figure 1D). To our knowledge, these are the first kinase structures in which the catalytic lysine is covalently modified by a sulfonyl fluoride-based inhibitor.

We next compared the ability of probes 1–3 to covalently modify endogenously expressed proteins in intact human cells. After treatment of Jurkat T cells with the probes (2 μM) for 30 min, lysates were prepared and subjected to click conjugation with rhodamine-azide. In-gel fluorescence analysis revealed that all three probes labeled many protein targets in common, with probe 2 displaying the strongest overall labeling intensity (Figure 2A). As a control for labeling specificity, cells were pretreated with probe variant 4 (20 μM), which lacks an alkyne, before adding the alkyne-tagged probes (Figure 2A). In samples pretreated

with 4, subsequent labeling of most proteins was abolished or strongly reduced. Hence, while probes 1–3 appear to promiscuously react with a large set of cellular proteins, most of these labeling events are specific and saturable. The level of “specific promiscuity” evidenced by Figure 2A is remarkable, and we are not aware of any pan-kinase probes that specifically modify so many proteins in cells and with such high signal-to-background.

To identify the probe-labeled proteins, we turned to affinity enrichment and mass spectrometry. As in the rhodamine-labeling experiment described above, live Jurkat cells were treated with probes 1–3 (2 μM) for 30 min (duplicate samples). After preparation of cell lysates at 4 °C, probe-labeled proteins were conjugated to biotinazide and purified with magnetic streptavidin beads (see Supporting Information for detailed methods). Enriched proteins were then subjected to on-bead trypsinization and the released peptides analyzed by LC–MS/MS. Consistent with the higher labeling intensity observed by in-gel fluorescence (Figure 2A), probe 2 captured 133 protein kinases (identified with ≥1 unique peptide, Supporting Information Table 1), substantially more than probes 1 and 3 (98 and 76 kinases, respectively). Most of the identified kinases were captured by at least two probes, with ~50% identified by all three probes, as expected given their shared recognition scaffold (Figure 2B and Supporting Information Table 1). Two of the kinases we identified, WNK1 and the pseudokinase STRADA, do not have a lysine in the same position as the catalytic lysine found in conventional protein kinases. However, structural analysis suggests that the sulfonyl fluoride probes could potentially react with proximal lysines found in WNK1 (Lys233, see PDB: 5tf9) and STRADA (Lys197 or Lys239, see PDB: 2wtk).

Despite comprising only 10–15% of the total number of proteins identified by mass spectrometry, kinases contributed two-thirds of the total ion intensity. Moreover, the median MS signal intensity across all identified kinases was ~10-fold higher than that of nonkinase proteins (Figure S3 and Supporting Information Table 2). Kinases are therefore the most abundant class of captured proteins based on MS signal intensity. Control experiments indicated that most of the nonkinase signal is probe-independent, likely due to nonspecific binding of abundant proteins to the streptavidin beads.

On the basis of its ability to capture the greatest number of kinases, we selected probe 2 (also referred to as XO44) to address the critical issue of kinase quantitation. Supporting the overall robustness and reproducibility of our label-free MS quantitation method, MS signal intensities for individual kinases were strongly correlated ($r^2 = 0.96$, $m = 1.18$) between two biological replicates (Figure 3A and Supporting Information Table 2). To confirm specific and saturable labeling of individual kinases, we used compound 4 as a competitor. Pretreatment of cells with 4 at 1 or 5 μM resulted in a concentration-dependent decrease in MS signal intensity for all kinases (Figure 3B,C and Supporting Information Table 2), consistent with in-gel fluorescence analysis performed in parallel (Figure S4). By contrast, most nonkinase proteins were unaffected. For 90% of identified kinases, pretreatment with 5 μM competitor 4 reduced MS signal intensity by more than 10-fold. Thus, when added to cells at 1–5 μM, compound 4 (and by extension, probe 2) is able to effectively compete with 1000-fold higher concentrations of ATP and covalently modify most of its kinase targets to >90% saturation within 30 min.

Having a cell-permeable occupancy probe enabled us to monitor intracellular kinase engagement by dasatinib, an approved drug for chronic myeloid leukemia that potently inhibits the BCR-ABL oncoprotein. Although dasatinib has been shown to inhibit many kinases in addition to BCR-ABL,[3,9,23] the extent of kinase occupancy achieved by therapeutically relevant concentrations in live cells is unknown. For assessment of dasatinib–kinase interactions in vivo, Jurkat cells were treated for 1 h with 100 or 300 nM dasatinib (or DMSO control), bracketing the maximum plasma concentrations measured in clinical trials.[24,25] After incubation with dasatinib, the cells were treated with probe 2 (2 μM, 30 min); cell lysates were then prepared and processed for streptavidin-bead enrichment and LC–MS/MS analysis.

Kinase intensity changes in response to dasatinib treatment (expressed as a percentage of DMSO control samples) were calculated from three independent experiments (Supporting Information Table 3). Using a stringent cutoff for statistical significance ($P < 0.0001$), we identified only 6 kinases that were occupied by >50% at 100 or 300 nM dasatinib (Figure 4A,B). Among these kinases, ABL1, BLK, and SRC were the most sensitive, as they were completely blocked by 100 nM dasatinib (100% inhibition of probe 2 labeling). By contrast, LCK occupancy was only 70% and 90% at 100 and 300 nM dasatinib, respectively; these differences were highly reproducible across 3 independent replicates. Probe 2-mediated capture of several other kinases known to be essential for T-cell proliferation and differentiation (e.g., ZAP70, ITK, JAK1, MAPK1, and AURKB) was not significantly affected by dasatinib. The partial occupancy of LCK under conditions in which dasatinib completely saturates BLK and SRC is surprising given the high sequence similarity shared by all 3 kinases (~70% identity). Indeed, previous biochemical studies,[3,23] including one that utilized kinobeads in Jurkat cell lysates,[26] concluded that dasatinib binds LCK and SRC with equal potency. Thus, by monitoring kinase engagement in live cells, we have uncovered a previously unappreciated ability of dasatinib to partially discriminate among related SRC-family kinases. One possibility is that dasatinib dissociates more rapidly from LCK than SRC in Jurkat cells. Because probe 2 saturates many kinases (Figure 3B,C and Supporting Information Table 2), a potential caveat is that dasatinib/kinase complexes with fast dissociation and slow rebinding kinetics may be difficult to detect and quantify with our method.

One of the challenges in quantifying inhibitor–kinase interactions in dilute lysates is the need to extrapolate potencies to the crowded, dynamic, and ATP-replete environment of the cell, usually without any direct knowledge of the inhibitor's intracellular concentration. In the aforementioned kinobeads study, for example, dasatinib IC_{50} measurements in ATP-depleted lysates were extrapolated to intracellular conditions (2 mM ATP) based on experimentally determined ATP binding affinities for each kinase. However, the extrapolated IC_{50}'s for LCK and SRC (0.5 and 1.0 μM, respectively)[26] drastically underestimate dasatinib's cellular potency based on previous measurements of downstream signaling, as well as our target engagement experiment ($IC_{50} \ll 100$ nM, Figure 4).[27–29]

As an alternative approach to evaluating the kinome coverage of probe 2, we tested it at 1 μM in enzymatic assays using purified kinases (Invitrogen kinase panel, Supporting Information Table 4). Of the 375 protein kinases tested, 219 were inhibited by ≥50%,

including 134 kinases that were not captured by probe 2 in Jurkat cells. Included in this latter set are several known dasatinib targets that are apparently not expressed in Jurkat cells (according to kinobead analysis, e.g., LYN, HCK, BTK, EPHA1, and SIK1).[26] Although not proven by the enzyme inhibition data (percent inhibition at 1 μM and a single time point of 1 h), we speculate that most of these kinases are susceptible to covalent modification. In principle, this expanded set of kinases (Figure S5) can be captured by probe 2 in cellular occupancy experiments, provided they are expressed at sufficient levels in the cells under investigation.

CONCLUSIONS AND PERSPECTIVE

The lysine-targeted sulfonyl fluorides reported in this study are, to our knowledge, the first probes that enable broad-spectrum assessment of kinase engagement in intact cells. Probe 2 (XO44, to be commercially available from Sigma-Aldrich) covalently labels up to 133 phylogenetically diverse kinases (Figure 5) when applied to a single cell line. Remarkably, 50 kinases that were captured by XO44 in live Jurkat cells were not captured by kinobeads in Jurkat cell lysates.[26] XO44 can therefore be used to complement chemoproteomic experiments carried out with kinobeads and ATP-biotin probes, with the added advantage of being cell permeable. Nevertheless, many predicted human kinases were not detected in Jurkat cells treated with XO44, leaving room for improvement in future work. We envision at least three strategies to address this challenge. The simplest, which is also the main strategy used in the kinobead and ATP-biotin platforms, is to use additional cell lines (i.e., non-T-cell lines) expressing distinct kinase subsets. On the basis of enzymatic assays with purified kinases, it is likely that XO44 has the potential to capture up to ~60% of the human kinome. A second strategy is to design orthogonal sulfonyl-fluoride-based probes based on distinct kinase-recognition scaffolds. Finally, future efforts will seek to improve the sensitivity of kinase quantitation through advanced instrumentation and proteomic methods, [30] including the use of parallel reaction monitoring.

Supplementary Material

Refer to Web version on PubMed Central for supplementary material.

Acknowledgments

Funding for this study was provided by HHMI (J.T.) and Pfizer. We thank Anatoly Urisman, Robert J. Chalkley, and Shenheng Guan for help with label-free MS quantitation; Erik Hett, Hendrik Neubert, and Simeon Ramsey for chemoproteomics advice; Robert Kyne, Jr., for synthetic intermediates; Rose Ann Ferre for help with EGFR crystallography; Todd VanArsdale and Sergei Timofeevski for help with kinase profiling. Mass spectrometry was provided by the UCSF Bio-Organic Biomedical Mass Spectrometry Resource supported by the Biomedical Technology Research Centers program (NIH NIGMS 8P41GM103481) and the Adelson Medical Research Foundation (A.L.B.).

References

1. Hu Y, Furtmann N, Bajorath J. J Med Chem. 2015; 58:30. [PubMed: 25051177]
2. Arrowsmith CH, Audia JE, Austin C, Baell J, Bennett J, Blagg J, Bountra C, Brennan PE, Brown PJ, Bunnage ME, Buser-Doepner C, Campbell RM, Carter AJ, Cohen P, Copeland RA, Cravatt B, Dahlin JL, Dhanak D, Edwards AM, Frederiksen M, Frye SV, Gray N, Grimshaw CE, Hepworth D, Howe T, Huber KVM, Jin J, Knapp S, Kotz JD, Kruger RG, Lowe D, Mader MM, Marsden B,

Mueller-Fahrnow A, Muller S, O'Hagan RC, Overington JP, Owen DR, Rosenberg SH, Ross R, Roth B, Schapira M, Schreiber SL, Shoichet B, Sundstrom M, Superti-Furga G, Taunton J, Toledo-Sherman L, Walpole C, Walters MA, Willson TM, Workman P, Young RN, Zuercher WJ. Nat Chem Biol. 2015; 11(11):536. [PubMed: 26196764]

3. Karaman MW, Herrgard S, Treiber DK, Gallant P, Atteridge CE, Campbell BT, Chan KW, Ciceri P, Davis MI, Edeen PT, Faraoni R, Floyd M, Hunt JP, Lockhart DJ, Milanov ZV, Morrison MJ, Pallares G, Patel HK, Pritchard S, Wodicka LM, Zarrinkar PP. Nat Biotechnol. 2008; 26:127. [PubMed: 18183025]
4. Fabian MA, Biggs WH, Treiber DK, Atteridge CE, Azimioara MD, Benedetti MG, Carter TA, Ciceri P, Edeen PT, Floyd M, Ford JM, Galvin M, Gerlach JL, Grotzfeld RM, Herrgard S, Insko DE, Insko MA, Lai AG, Lelias J-M, Mehta SA, Milanov ZV, Velasco AM, Wodicka LM, Patel HK, Zarrinkar PP, Lockhart DJ. Nat Biotechnol. 2005; 23:329. [PubMed: 15711537]
5. Ku X, Heinzlmeir S, Helm D, Médard G, Kuster B. J Proteome Res. 2014; 13:2445. [PubMed: 24712744]
6. Ku X, Heinzlmeir S, Liu X, Médard G, Kuster B. J Proteomics. 2014; 96:44. [PubMed: 24184958]
7. Pachl F, Plattner P, Ruprecht B, Médard G, Sewald N, Kuster B. J Proteome Res. 2013; 12:3792. [PubMed: 23795919]
8. Zhang L, Holmes IP, Hochgräfe F, Walker SR, Ali NA, Humphrey ES, Wu J, de Silva M, Kersten WJA, Connor T, Falk H, Allan L, Street IP, Bentley JD, Pilling PA, Monahan BJ, Peat TS, Daly RJ. J Proteome Res. 2013; 12:3104. [PubMed: 23692254]
9. Bantscheff M, Eberhard D, Abraham Y, Bastuck S, Boesche M, Hobson S, Mathieson T, Perrin J, Raida M, Rau C, Reader V, Sweetman G, Bauer A, Bouwmeester T, Hopf C, Kruse U, Neubauer G, Ramsden N, Rick J, Kuster B, Drewes G. Nat Biotechnol. 2007; 25:1035. [PubMed: 17721511]
10. Patricelli MP, Szardenings AK, Liyanage M, Nomanbhoy TK, Wu M, Weissig H, Aban A, Chun D, Tanner S, Kozarich JW. Biochemistry. 2007; 46:350. [PubMed: 17209545]
11. Patricelli MP, Nomanbhoy TK, Wu J, Brown H, Zhou D, Zhang J, Jagannathan S, Aban A, Okerberg E, Herring C, Nordin B, Weissig H, Yang Q, Lee J-D, Gray NS, Kozarich JW. Chem Biol. 2011; 18:699. [PubMed: 21700206]
12. Shi H, Zhang C-J, Chen GYJ, Yao SQ. J Am Chem Soc. 2012; 134:3001. [PubMed: 22242683]
13. Ranjitkar P, Perera BGK, Swaney DL, Hari SB, Larson ET, Krishnamurty R, Merritt EA, Villén J, Maly DJ. J Am Chem Soc. 2012; 134:19017. [PubMed: 23088519]
14. Narayanan A, Jones LH. Chem Sci. 2015; 6:2650. [PubMed: 28706662]
15. Dong J, Krasnova L, Finn MG, Sharpless KB. Angew Chem, Int Ed. 2014; 53:9430.
16. Grimster NP, Connelly S, Baranczak A, Dong J, Krasnova LB, Sharpless KB, Powers ET, Wilson IA, Kelly JW. J Am Chem Soc. 2013; 135:5656. [PubMed: 23350654]
17. Colman RF. Annu Rev Biochem. 1983; 52:67. [PubMed: 6311082]
18. Gushwa NN, Kang S, Chen J, Taunton J. J Am Chem Soc. 2012; 134:20214. [PubMed: 23190395]
19. Statsuk AV, Maly DJ, Seeliger MA, Fabian MA, Biggs WH, Lockhart DJ, Zarrinkar PP, Kuriyan J, Shokat KM. J Am Chem Soc. 2008; 130:17568. [PubMed: 19053485]
20. Aronov AM, Murcko MA. J Med Chem. 2004; 47:5616. [PubMed: 15509160]
21. Hett EC, Xu H, Geoghegan KF, Gopalsamy A, Kyne RE, Menard CA, Narayanan A, Parikh MD, Liu S, Roberts L, Robinson RP, Tones MA, Jones LH. ACS Chem Biol. 2015; 10:1094. [PubMed: 25571984]
22. Gu C, Shannon DA, Colby T, Wang Z, Shabab M, Kumari S, Villamor, Joji G, McLaughlin, Christopher J, Weerapana E, Kaiser M, Cravatt, Benjamin F, van der Hoorn, Renier AL, et al. Chem Biol. 2013; 20:541. [PubMed: 23601643]
23. Das J, Chen P, Norris D, Padmanabha R, Lin J, Moquin RV, Shen Z, Cook LS, Doweyko AM, Pitt S, Pang S, Shen DR, Fang Q, de Fex HF, McIntyre KW, Shuster DJ, Gillooly KM, Behnia K, Schieven GL, Wityak J, Barrish JC. J Med Chem. 2006; 49:6819. [PubMed: 17154512]
24. Johnson FM, Bekele BN, Feng L, Wistuba I, Tang XM, Tran HT, Erasmus JJ, Hwang L-L, Takebe N, Blumenschein GR, Lippman SM, Stewart DJ. J Clin Oncol. 2010; 28:4609. [PubMed: 20855820]

25. Christopher LJ, Cui D, Wu C, Luo R, Manning JA, Bonacorsi SJ, Lago M, Allentoff A, Lee FYF, McCann B, Galbraith S, Reitberg DP, He K, Barros A, Blackwood-Chirchir A, Humphreys WG, Iyer RA. Drug Metab Dispos. 2008; 36:1357. [PubMed: 18420784]

26. Becher I, Savitski MM, Savitski MF, Hopf C, Bantscheff M, Drewes G. ACS Chem Biol. 2013; 8:599. [PubMed: 23215245]

27. Lee KC, Ouwehand I, Giannini AL, Thomas NS, Dibb NJ, Bijlmakers MJ. Leukemia. 2010; 24:896. [PubMed: 20147973]

28. Blake S, Hughes TP, Mayrhofer G, Lyons AB. Clin Immunol. 2008; 127:330. [PubMed: 18395492]

29. Schade AE, Schieven GL, Townsend R, Jankowska AM, Susulic V, Zhang R, Szpurka H, Maciejewski JP. Blood. 2008; 111:1366. [PubMed: 17962511]

30. Urisman A, Levin RS, Gordan JD, Webber JT, Hernandez H, Ishihama Y, Shokat KM, Burlingame AL. Mol Cell Proteomics. 2016 mcp.M116.058172.

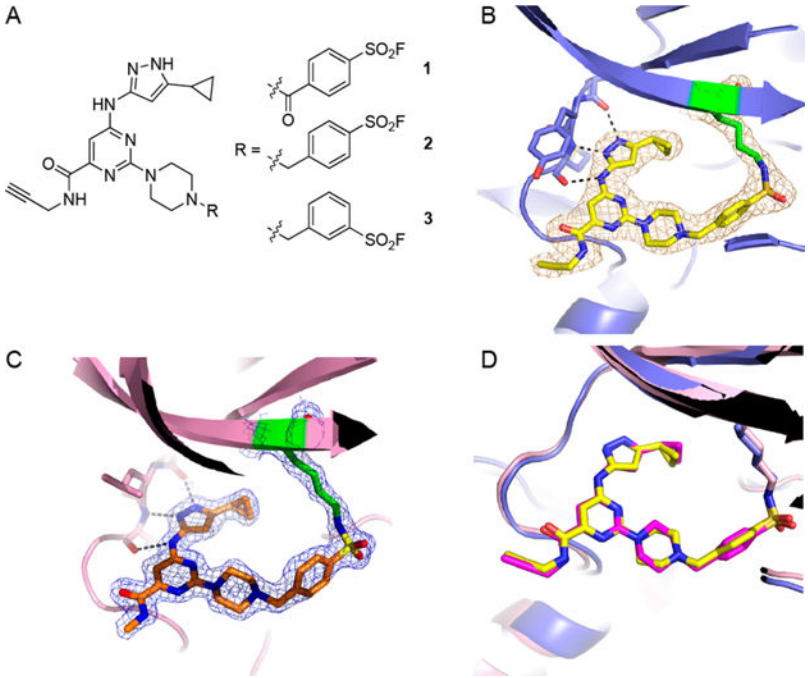

Figure 1.

(A) Sulfonyl fluoride probes derived from a pyrimidine 2-aminopyrazole kinase-recognition scaffold. (B, C) Cocrystal structures showing probe 2-modified kinase domains of SRC (B) and EGFR (C). Electron density maps ($2F_o - F_c$) are shown at a contour level of 1σ. (D) Overlay of probe 2-modified SRC and EGFR structures. SRC: 2 in yellow, Lys295 in blue. EGFR: 2 in magenta, Lys745 in pink.

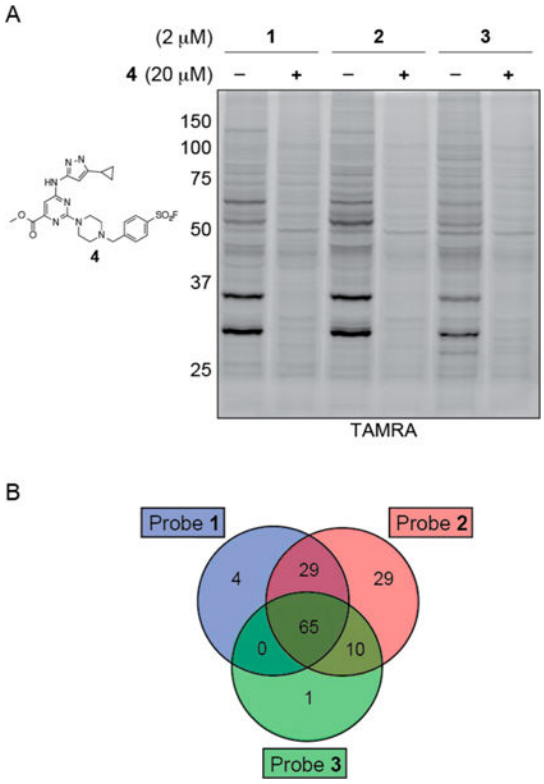

Figure 2.

Probes 1–3 label multiple endogenous protein kinases in live cells. (A) Jurkat cells were treated with either DMSO or nonclickable competitor 4 (20 μM) for 1 h, followed by probes 1–3 (2 μM) for 30 min. Cell lysates were subjected to click chemistry with rhodamine-azide, resolved by SDS-PAGE, and scanned for fluorescence (TAMRA). (B) Venn diagram showing the number of shared and unique kinases identified by LC–MS/MS after treatment of Jurkat cells with probes 1–3 (2 μM, 30 min).

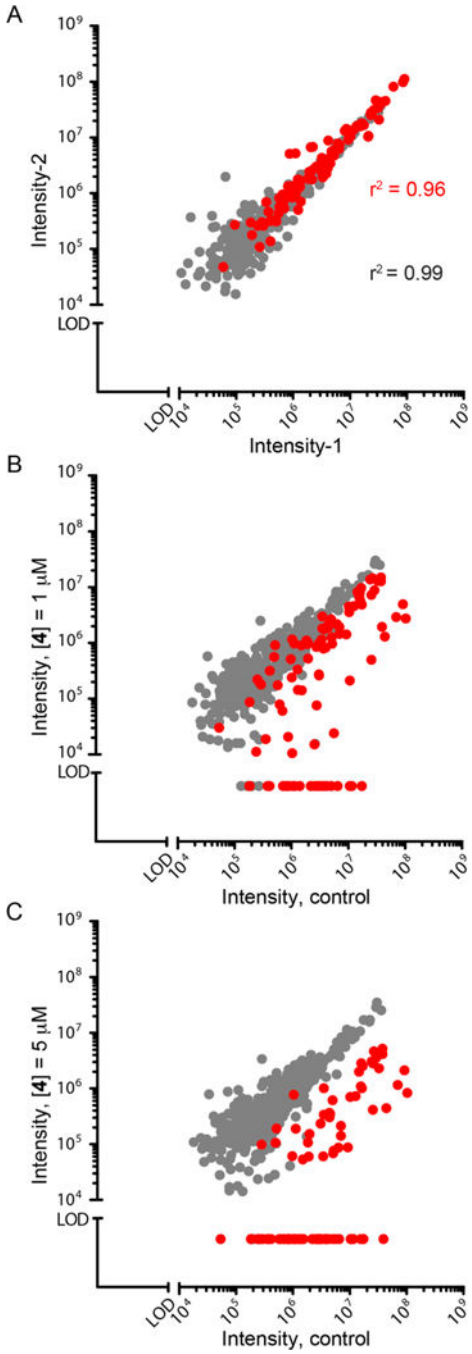

Figure 3.

Scatter plots showing MS signal intensities for individual kinases (red dots) and nonkinases (gray dots) identified in chemoproteomic experiments with probe 2 (Supporting Information Table 2). The MS signal intensity for each protein was calculated as the sum of intensities from each unique peptide. (A) Jurkat T cells were treated with probe 2 (2 μM, 30 min). MS signal intensities from two biological replicates (intensity-1 and intensity-2) are plotted to demonstrate reproducibility. (B) *Y*-axis: cells were pretreated with competitor 4 (1 μM, 1 h), followed by treatment with probe 2. *X*-axis: control cells treated with probe 2. (C) As in part

B, except cells were pretreated with 4 at 5 μM. Pretreatment with 4 reduces signal intensity in a concentration-dependent manner for most kinases, but only a few nonkinases. LOD = limit of detection.

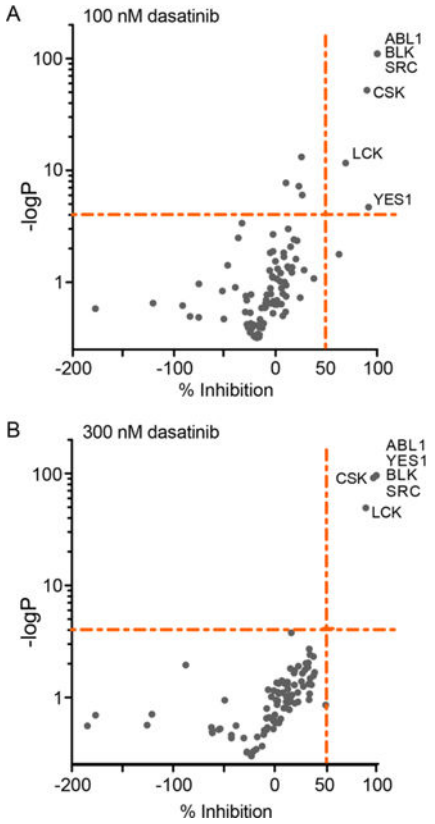

Figure 4.

(A) Volcano plot showing MS signal intensities for probe 2-captured kinases from cells pretreated with 100 nM dasatinib as a percentage of the signal from control cells pretreated with DMSO (mean from 3 experimental replicates, Supporting Information Table 3). The *Y*-axis depicts the −log *P* value for each quantified kinase (threshold of significance, $P < 0.0001$). (B) As in part A, except cells were pretreated with 300 nM dasatinib.

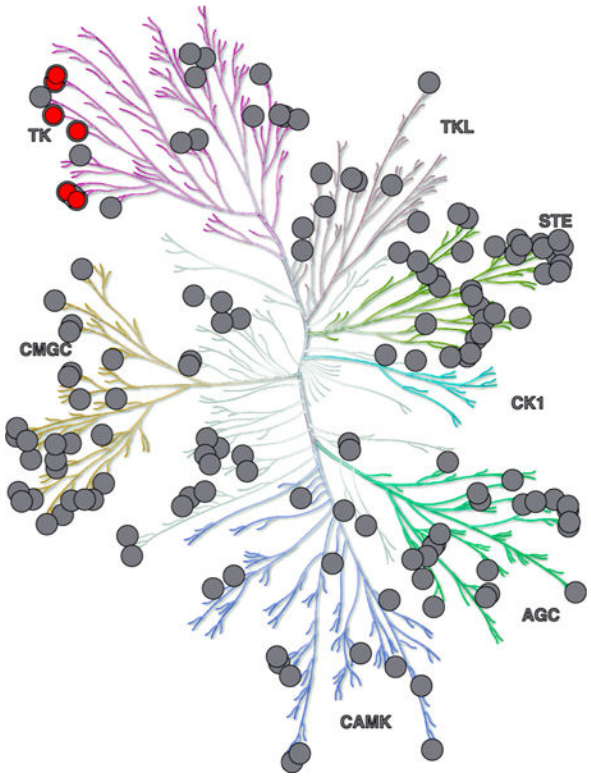

Figure 5.

Kinome coverage of probe 2 based on chemoproteomic experiments in Jurkat cells. All major branches of the kinome tree are covered. Red dots indicate kinases showing significant occupancy after treating cells with 100 or 300 nM dasatinib (see Figure 4).